Current Biology, Vol. 12, 1718–1727, October 15, 2002, ©2002 Elsevier Science Ltd. All rights reserved. PII S0960-9822(02)01151-X

# *EXS*, a Putative LRR Receptor Kinase, Regulates Male Germline Cell Number and Tapetal Identity and Promotes Seed Development in *Arabidopsis*

**Claudia Canales,[1] Anuj M. Bhatt,[1] Rod Scott,[2] and Hugh Dickinson[1,3]**

[1]Department of Plant Sciences
South Parks Road
University of Oxford
Oxford OX1 3RB

[2]Department of Biology and Biochemistry
University of Bath
Bath BA2 7AY
United Kingdom

## Summary

**Background:** Plant germlines arise late in development from archesporial initials in the L2 layer of the anther and ovule primordia. These cells generate a radially symmetrical array of tissues that, in the *Arabidopsis* anther, comprises a core of sporogenous cells (meiocytes) and the enveloping tapetum, middle cell, and endothecium layers. The putative transcription factor *NZZ/SPL* [1, 2] is required for the specification of archesporial cells, but nothing is known of how their number is regulated, or what controls cell fate in the lineages they generate. Here, we report detailed characterization of *extra sporogenous cells* (*exs*), a male sterile mutant that generates extra meiocytes but lacks tapetal and middle cell layers [3, 4].

**Results:** We identified the *EXS* locus by map-based cloning and found it to encode a putative LRR receptor kinase. In the anther, an increased number of L2 layer cells assume an archesporial fate and divide to generate a larger number of sporogenous cells. In seeds, the *exs* mutation results in smaller embryonic cells, delayed embryo development, and smaller mature embryos. Consistent with the observed phenotype, *EXS* is expressed in the inflorescence meristem, floral apices, anthers, and in developing seeds.

**Conclusions:** *EXS* regulates the number of cells that divide in the L2 layer of the anther, and thus the number of functional male archesporial initials. In the young seed, *EXS* affects cell size in the embryo and the rate at which it develops. The apparently contrasting roles of *EXS* in the anther and embryo suggest that signaling through the *EXS* receptor kinase is a feature of a number of regulatory pathways in *Arabidopsis*.

## Introduction

Unlike in animals, where primordial germ cell specification is an early embryonic event, in plants reproductive organs and their germlines differentiate late in development. Within the developing anthers and ovules, the cell lines giving rise to the male and female sporogenous cells (meiocytes) are generated de novo from the hypodermal L2 layer. In the *Arabididopsis* anther, four of these cells develop in the position subsequently occupied by the microsporangia, while a single distal sporogenous cell is formed in the ovule. Archesporial cells develop very differently according to their sex. In anthers, each of the four archesporial initials undergoes a series of periclinal divisions to form the primary sporogenous cells and the radial anther wall cell layers — the endothecium, middle cell, and nutritive tapetum. These cell types form the microsporangium in which the sporogenous cells continue their development first into microspores, and then into multinucleate pollen grains. In the ovule, the single archesporial cell enters meiosis directly, and one of the four meiotic products undergoes a series of divisions leading to the formation of the female gametophyte — the embryo sac. The embryo sac contains the egg cell, a central cell (which fuses with one of the two sperms to form the endosperm), and other cells involved in the reception of the pollen tube and nutrition of the embryo sac itself. Therefore, a second key difference between animal and plant germ cells is that plant meiocytes generate a haploid gametophytic generation, while, in animals, germ cells produce gametes directly. Anthers and ovules are thus not only the sites of the switch from mitotic to meiotic development, but they are also the sites of the transition from diploid sporophytic to haploid gametophytic generations.

Although progress has recently been made in understanding the control of ovule development [5–7], little is known of the molecular regulation of anther formation. Certainly, a number of genes affect development of both sex organs; for example, *STERILE APETALA* (*SAP*) encodes a transcription factor required for inflorescence, floral, and ovule development [8]. Interestingly, *sap* mutant plants have sterile, abnormally differentiated anthers, suggesting that *SAP* is required for anther development [8]. Aberrant anther development has also been reported in plants lacking the wild-type function of the *TSO1* gene [9, 10]. However, the genes responsible for the specification of the tissues within anthers remain largely unknown. A notable exception is the putative transcription factor *NOZZLE/SPOROCYTELESS* (*NZZ/SPL*) [1, 2], which is expressed in both male and female tissues and is required for archesporial cell development. The question still remains of how archesporial development is restricted to four cells in the anther and a single distal cell in the ovule.

We recently described a male sterile mutant of *Arabidopsis*, generically termed *gne2* (*gus-negative2*) [3, 4], with disrupted anther development. Plants carrying the *gne2* mutation produce an increased number of sporogenous cells in anthers but form neither tapetal nor middle cell layers. We therefore renamed the mutation *extra sporogenous cells* (*exs*). *exs* mutant sporogenous cells develop until the tetrad stage during meiosis II, when cell degeneration occurs. We have now cloned and characterized in detail three mutant alleles of *EXS*. *EXS* encodes a putative leucine-rich repeat (LRR) receptor kinase and is expressed in floral meristems, anthers,

[3]Correspondence: hugh.dickinson@plants.ox.ac.uk

ovules, and developing seeds. Here, we present evidence that the *exs* phenotype is the result of increased cell division in the L2 layer of developing anthers. *EXS* therefore is required for the specification of the correct number of male archesporial initials and for the subsequent specification of tapetal and middle cell layer identities. *EXS* does not only affect the development of reproductive cells, as *exs* embryos also develop more slowly, contain smaller cells, and form seeds strikingly reduced in size.

## Results

### Cell Lineage in the *Arabidopsis* Anther

A clear picture of the cell lineages leading to the tissues of the microsporangium is central to understanding how *EXS* regulates cell number and fate in the anther. Detailed descriptions exist in the recent literature (e.g., [2, 11]), but data from an extensive cytological study of wild-type anthers, and the *exs* mutant itself, suggest that some reinterpretation of these accounts is required (see Figure 1). At anther development stage 7 [12], single archesporial cells arise in the L2 layer at points subsequently occupied by the four microsporangia. These divide periclinally (Figure 2A) to form an inward-facing primary sporogenous (PS) cell and a primary parietal cell (PP) facing the outside of the anther. The PP then divides periclinally to form inner secondary parietal cells (ISP) and an outer secondary parietal layer (OSP) that develops into the endothecium (Figures 2C, 2E, 2G, and 2I). Later in anther development, the endothecium plays a major part in dehiscence. In a final periclinal division, the ISP divides to form a tapetal cell next to the developing meiocytes and a middle layer cell beneath the endothecium (Figures 2C and 2E). The nature of these last two divisions clearly differs between species, as, in other genera, the sporogenous and tapetal cells are formed in the same periclinal division [13]. While this lineage is correct for the direct descendants of the archesporial cells, it cannot explain the formation of the complex concentric organization of the microsporangial layers. This evolves during the divisions described above and may result from gradients of positional information, presumably generated from the sporogenous cells, which guide adjacent, anticlinally dividing cell layers into tapetal, middle, and endothecial cell fates. The final number of sporogenous cells is attained by a mitotic division of the primary sporogenous cells once anther wall layer development is complete, before the onset of meiosis (compare Figures 2E and 2G).

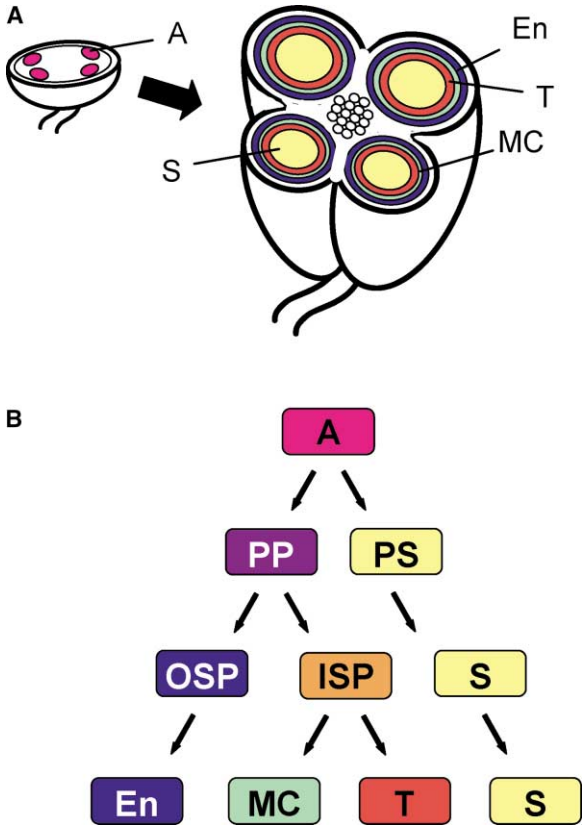


Figure 1. Model of Anther Development in *Arabidopsis*

(A) Specification of the subepidermal archesporial initials in the four corners of the anther primordium. Archesporial initials divide to generate the central sporogenous cell mass and the investing anther wall layers — tapetum, middle cell, and endothecium — on the epidermal side of each anther locule. The inner portion of the anther wall layer is the result of divisions of the connective.

(B) Division of the archeosporial initials during anther development. Each archeosporial initial divides in periclinal orientation to produce an inner primary sporogenous layer and an outer primary parietal layer. The primary sporogenous cell layer gives rise to the central mass of sporogenous cells, while the primary parietal layer generates an outer secondary parietal and an inner secondary parietal layer. The endothecium is derived from the former, while the tapetal and middle cell layers develop from the inner secondary parietal layer. Abbreviations: A, archesporial initials; En, endothecium; ISP, inner secondary parietal layer; MC, middle cell layer; OSP, outer secondary parietal layer; PP, primary parietal cell layer; PS, primary sporogenous cell layer; S, sporogenous cells; T, tapetum.

### *EXS* Controls the Number and Position of Periclinal Cell Divisions in the L2 Layer of Anther Primordia

Three families carrying different mutant alleles of *EXS* (*exs-1*, *exs-2*, *exs-3*) have been subject to phenotypic and molecular characterization. We observed no differences between the three available *exs* alleles in anther development. In all three mutants, anthers at stage 8 [12] possess an increased number of sporogenous cells. While precise counts are difficult to obtain, transverse sections of *exs* anthers transect 8–11 sporocytes, while only 3–5 of these cells are transected in wild-type plants (see Figures 2 and 4 in [4]; compare Figures 2G and 2H in this report). Further, the mutant anthers possess no organized tapetal and middle cell layers, and this phenotype is most severe on the inward-facing microsporangial surface (Figure 2J) that is adjacent to the anther connective.

Our data clearly demonstrate that the extra sporogenous cells phenotype results from the specification of extra archesporial initials. Detailed cytological analysis of wild-type and *exs* anther development reveals that, in the mutant, a greatly increased number of L2 cells undergoes anticlinal divisions to form PSs and PPs (Figure 2B). Not all L2 cells develop in this way, for the

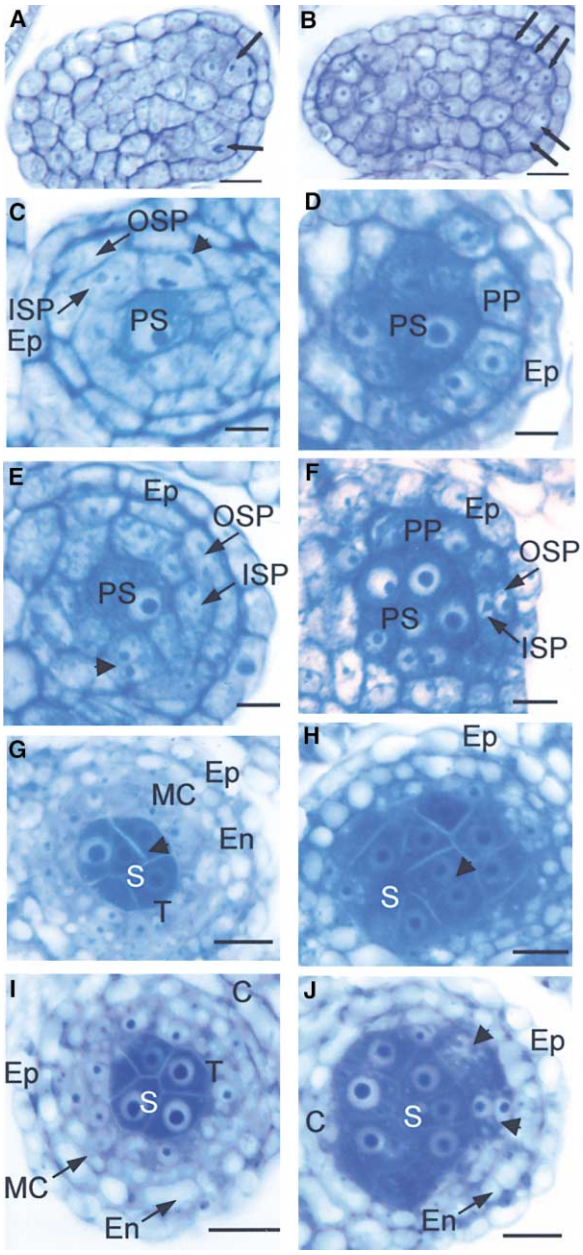


Figure 2. Anther Development in *exs* Mutant Plants

Micrographs of wild-type and *exs* mutant anther sections stained with toluidine blue.

(A) Archesporial initial division (arrows) in a wild-type anther primordium. Only two archesporial cells are visible due to the orientation of the sample.

(B) In *exs* mutant anthers, increased cell division in the L2 cell layer of anther primordia results in the specification of a larger number of archesporial initials (arrows).

(C) Division of the ISP layer in a wild-type locule to generate the tapetal and middle cell layers. The arrowhead points to a cell of the ISP in mitotic anaphase.

(D) An *exs* mutant locule showing the increased number of primary sporogenous cells specified (four observable in this section), and the primary parietal layer.

(E) A wild-type anther locule showing one primary sporogenous cell and the secondary parietal layers. The arrowhead points to a cell in the ISP layer with two nuclei, prior to mitotic cytokinesis.

(F) An *exs* anther locule with four primary sporogenous cells; the region where the primary parietal layer has divided to generate the secondary wall layers is marked by arrows.

(G) A premeiotic wild-type anther locule; subsequent to the formation of the anther wall layers, and before the onset of meiosis, the primary sporogenous cells undergo a mitotic division and attain their final number. The arrowhead points to a new wall formed after division of an SP.

(H) In *exs*, the premeiotic division of the primary sporogenous cells takes place as in wild-type, thereby producing the final number of *exs* sporogenous cells.

(I) A premeiotic wild-type anther locule showing the central mass of sporogenous cells and the investing anther wall layers: tapetum, middle cell layer and endothecium.

(J) In *exs* mutant anthers, a larger number of sporogenous cells is specified, and anther wall development is aberrant. Organized tapetal and middle cell layers are not formed, and the number of anther wall layers is variable. Few cells of unknown cell identity (arrowheads) usually develop on the epidermal side of *exs* anther locules, but they do not form a complete wall enclosing the sporogenous cells. The *exs* phenotype is most severe on the inner side of the anther locule, where sporogenous cells develop in direct contact to connective tissue. Abbreviations: C: connective; En: endothecium; Ep: epidermis; ISP: inner secondary parietal layer; MC: middle cell layer; OSP: outer secondary parietal layer; PP: primary parietal layer; PS: primary sporogenous cells; S: sporogenous cells; T: tapetum.

The scale bars represent 10 μm.

majority of the hypodermal cells of the ab- and adaxial faces of the anther remain unaffected. Nevertheless, in *exs* anthers, large numbers of adjacent L2 cells on the lateral surfaces assume an archesporial cell fate, compared with four in the wild-type anther. The primary sporogenous cells generated by this "layer" of archesporial cells (Figures 2D and 2F) then undergo the normal number of mitoses to reach their final number (Figures 2H and 2J), and they then enter meiotic prophase. Commitment to meiosis at the molecular level was confirmed by expression of the prophase-specific marker *AtDMC1* [14] in both wild-type and *exs* mutant anthers (data not shown). Male development subsequently proceeds through meiosis I and II to the tetrad stage in *exs* mutants, but there is evidence of increasing cytoplasmic disruption [4] and aberrant accumulation of the β1-3 glucan, callose, which normally invests the meiocytes (compare Figures 3A and 3C with Figures 3B and 3D). Development ceases at the tetrad stage when the germline degenerates; mature anthers contain a perfect epidermis and endothecial layer, but no pollen.

There is no evidence of tapetal and middle layer development in *exs* mutants, and in situ hybridization with a tapetal-specific probe (*A9*; [15]) failed to detect expression in *exs* anthers (results not shown). The inner secondary parietal cells (ISPs), which would have given rise to the middle and tapetal layers in wild-type plants, either degenerate or are crushed between the sporogenous mass and the endothecium, or they remain as small indeterminate cells with no defining morphology.

### Development Is Delayed and Growth Is Inhibited in *exs* Seeds

*exs*/+ heterozygous plants are fertile but produce significantly smaller seeds (Figure 4C) in a ratio of 3:1 normal:small. Investigation of early seed development in these plants showed that these seeds are not only

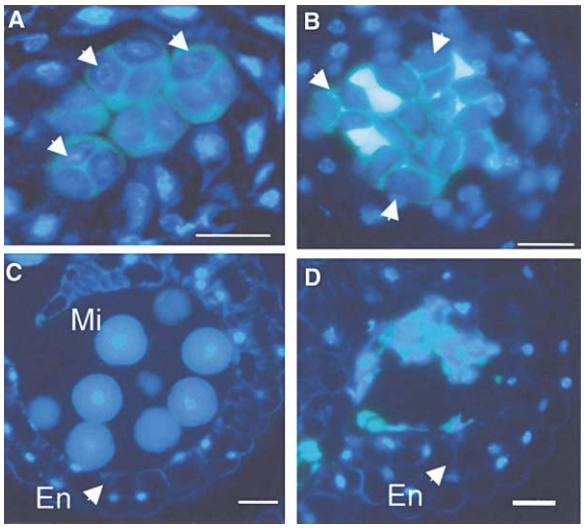


Figure 3. Male Meiosis in *exs*

Micrographs of wild-type and *exs* mutant anthers stained with DAPI for DNA and aniline blue for callose and viewed under UV light.
(A) Wild-type tetrads (cross-walls are indicated by arrowheads).
(B) *exs* mutant tetrads (cross-walls are indicated by arrowheads). Despite the abnormal anther wall development in *exs* mutant anthers, the early stages of meiosis appear normal. However, signs of cellular degeneration of *exs* sporogenous cells become evident from meiosis II onward. Note the abnormal pattern of callose deposition in mutant anthers.
(C) A wild-type anther locule with mature pollen grains, after pollen mitosis I. The degradation of the tapetal layer is complete.
(D) In *exs* mutant plants, mature anthers lack pollen. Anther locules are filled with callose masses and the cellular remains of the sporogenous cells. However, endothecium development in *exs* appears normal. Abbreviations: En: endothecium; Ep: epidermis; MC: middle cell layer; Mi: microspores; S: sporogenous cells; T: tapetum.
The scale bars represent 10 μm.

smaller at maturity, but they also develop slowly. Similarly, confocal and light microscopy studies of seeds from the same silique of an *exs-2*/+ selfed plant reveal that the embryos of smaller seeds are significantly delayed in their development (Figures 4A, 4B, 4D, and 4E). Endosperm development also lags in the smaller seed class, for, by the time full cellularization has occurred in the larger seeds, the endosperm of the smaller seed class still remains coenocytic (Figures 4A and 4B).

The embryos of the two classes of mature seeds also differ significantly in size (Figure 4F). Cell number and size in these two classes of embryos were determined by measuring 200 cells from adjacent files on the hypocotyl surface of 20 embryos from each class (there is considerable variation between cell size in different files). The data showed that, while cell number was equivalent, cells of the larger embryos were themselves significantly larger (Figures 4G and 4H; Table 1). The overall organization of the two embryo classes was very similar, although the shoot apical meristem (SAM) and root apical meristem (RAM) were reduced in size in the smaller seeds (Figures 4I–4L). Upon germination, the smaller seeds initially gave rise to smaller seedlings, a difference that was lost after germination.

Germination and growth to reproductive maturity of the two seed classes confirmed that the smaller seeds were homozygous for the *exs-2* mutation.

### *EXS* Encodes a Putative LRR Receptor Kinase

We used positional cloning to identify the *EXS* gene (Figure 5A). Published and novel molecular markers were used to map *exs* within a 160-kb interval on the top arm of chromosome 5. A total of 28 putative ORFs were annotated in this region by the *Arabidopsis* Genome Initiative (http://www.Arabidopsis.org/agi.html). Individual ORFs were amplified from genomic DNA of wild-type C24 and *exs* alleles and were digested to detect mutant-specific polymorphisms. Analysis of the putative LRR receptor kinase *At5g07280* showed a mutant allele-specific polymorphism in *exs-3*. The three available *exs* alleles were sequenced and were found to have point mutations in this locus (Figures 5B and 5C). In *exs-1*, the mutation results in a glutamic acid to valine substitution in the catalytic kinase domain of the protein, while, in *exs-2*, a lysine residue substitutes for an asparagine in the second LRR. *exs-3* results from a premature stop codon in amino acid 249 and is considered to be a likely null allele. A total of 89 bp of the 5′ UTR of EXS were amplified by direct PCR using cDNA synthesized from DNA-free bud total RNA, while the 3′ UTR of *EXS* (160 bp long) was determined by RACE.

To provide further evidence that *At5g07280* corresponds to *EXS*, a 9.2-kb genomic fragment comprising the ORF and 3.5 kb and 2.2 kb of the upstream and downstream sequences, respectively, was transformed into *exs-2*/+ plants. Complemented *exs-2* plants were identified among the male fertile transformants by using a genetic marker polymorphic for wild-type C24, *exs-2,* and the transgene (details given in the Experimental Procedures). *35S:EXS* and in-frame *EXS-GUS* translational fusions were also found to complement *exs*. A comparison between genomic and cDNA sequences confirmed that the EXS ORF contains a single exon (GenBank accession number AJ496433). The predicted EXS protein contains 21 LRRs, a putative transmembrane domain, and a serine/threonine kinase catalytic domain (Figure 5C).

### *EXS* Is Expressed in Inflorescence and Floral Meristems, Developing Anthers and Ovules, and Seeds

*EXS* expression was investigated by using RT-PCR, in situ hybridization, *EXS* promoter (*pEXS*)-*GUS* transcriptional fusions, and *pEXS-EXS-GUS* translational fusions. RT-PCR (26 cycles) demonstrated that *EXS* transcript is present in young buds, open flowers, and siliques but is absent from mature leaves and roots (data not shown).

Both in situ and *GUS* fusion strategies showed that *EXS* is strongly expressed in the young anthers and ovaries (Figures 6 and 7). In situ hybridization revealed that *EXS* transcripts are present in the inflorescence meristem (Figure 6A) and in the developing floral meristems (Figure 6B). A strong in situ signal continued in the young organ primordia, which, as the anthers and ovules developed, became focused in the microsporangia (Figures 6C–6G) and in the distal and chalazal regions of the ovule (Figures 6H and 6I). In the anther, expression con-

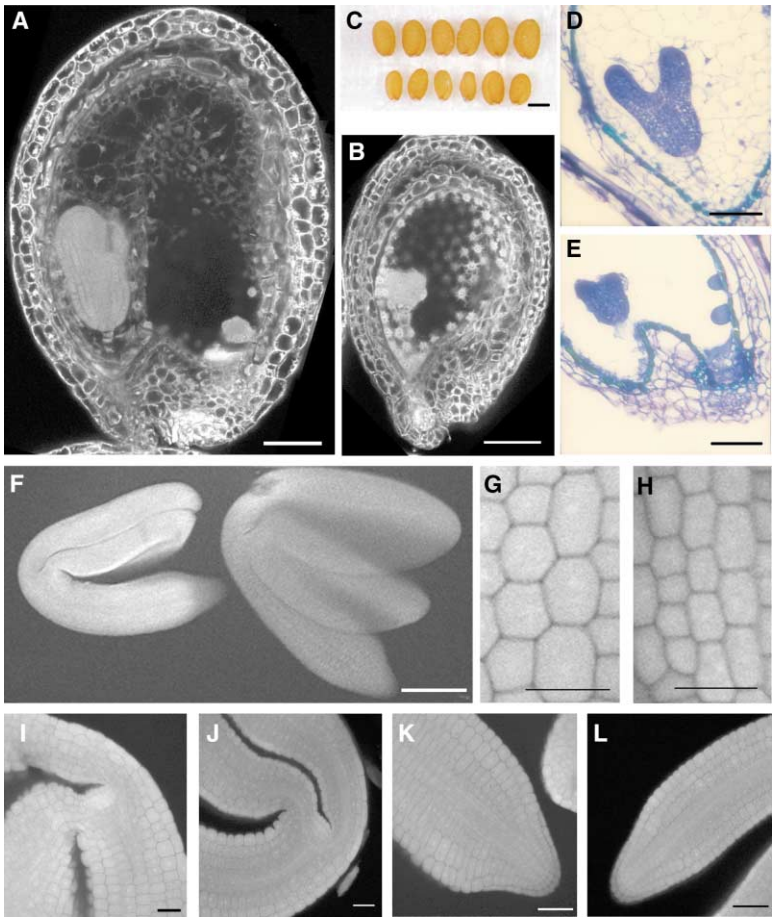


Figure 4. Seed Development in *exs*

(A and B) Confocal micrographs of (A) Feulgen-stained wild-type and (B) small *exs-2* seeds from the same silique of a plant heterozygous for *exs-2*, shown at the same magnification. Embryo and endosperm development of the smaller seed class is delayed in comparison to the development of their wild-type siblings. The endosperm in the large, wild-type seeds has cellularized, while, in *exs-2* seeds, it is still at the free-nuclear stage.

(C) A photograph of seeds derived from a selfed *exs-2*/+ parent. Small and large seeds segregate in a 1:4 ratio.

(D and E) Micrographs of sections of large and small seeds derived from the same *exs-2*/+ silique stained with toluidine blue.

(F–L) Confocal micrographs of mature embryos stained with anline blue. (F) The two classes of mature embryos produced in a selfed *exs-2*/+ plant viewed with confocal microscopy. (G and H) Hypocotyl epidermal cells in (G) wild-type and (H) *exs-2* mature embryos. (I–J) Apical meristems in wild-type and *exs-2* embryos. (K and L) Root meristems in wild-type and *exs-2* mature embryos.

The scale bar represents 60 μm in (A) and (B), 300 μm in (C), 100 μm in (D) and (E), 50 μm in (F) and (I)–(L), and 20 μm in (G) and (H).

tinued in the meiocytes and young pollen grains until pollen mitosis II (Figures 6E–6G). There was a strong signal in the tapetum while the meiocytes were undergoing meiosis I and II, but, afterwards, it began to attenuate and was markedly decreased by the uninucleate microspore stage (Figures 6E–6G).

Expression of the *pEXS-GUS* and *pEXS-EXS-GUS* fusions was consistent with the in situ hybridization data (Figures 7A–7C), but comparison of the expression patterns of the two fusion classes clearly shows that, while the *EXS* promoter directs expression in the young ovular primordia, the EXS-GUS protein is not present in these organs (compare Figures 7C and 7D). *pEXS-GUS* reporter gene expression was also used to investigate *EXS* expression in developing seeds (Figures 7E and 7F). *EXS* transcripts were present from the earliest stages in seed formation and were focused at the funicular pole (Figure 7E). Sections of these seeds show strong *EXS* expression in the young globular embryo (Figure 7F) and in the endosperm (data not shown). As the embryo develops, *EXS* transcripts become focused at the shoot and root meristems and in the early vasculature of the hypocotyl and cotyledons (Figure 7G; expression in root meristems is not shown). *EXS* activity continues as the seed germinates, with transcript present at the shoot meristem, in the basal meristems of the cotyledons, and in stipules (Figure 7H). *EXS* expression is lost from roots early in seedling development.

Table 1. Measurements of Mature Embryos and Embryonic Epidermal Cells in Wild-Type and Mutant *exs* Mutants

| Allele | Mean Hypocotyl Length | Mean Hypocotyl Epidermis Cell Area | Mean Hypocotyl Surface Length | Mean Hypocotyl Epidermis Cell Length | Mean Hypocotyl Surface Length/ Mean Hypocotyl Epidermis Cell Length |
|---|---|---|---|---|---|
| WT | 480.75 ± 9.18 μm | 234.68 ± 4.95 μm$^2$ | 598.05 ± 9.41 μm | 15.79 ± 0.28 μm | 37.87 |
| *exs-1* | 474.59 ± 8.37 μm | 178.59 ± 14.17 μm$^2$ | 567.91 ± 9.64 μm | 15.00 ± 0.27 μm | 37.86 |
| *exs-2* | 398.79 ± 10.63 μm | 140.45 ± 14.31 μm$^2$ | 486.85 ± 11.22 μm | 12.33 ± 0.25 μm | 39.48 |
| *exs-3* | 409.11 ± 11.31 μm | 140.31 ± 14.14 μm$^2$ | 529.27 ±13.16 μm | 13.30 ± 0.98 μm | 39.79 |

Loss of *exs* reduces organ and cell size in developing seeds. Confocal microscopy images of mature wild-type and *exs* mutant embryos were used to measure hypocotyl length and epidermal cell area and length. A total of 200 hypocotyl epidermal cells from adjacent root files were measured from 20 embryos for each sample. *exs-2* and *exs-3* embryos were found to be significantly smaller (~85% of wild-type; $p < 0.001$) and to have smaller cells (~60% of wild-type; $p < 0.001$), while *exs-1* embryos show a less severe reduction in size.

A

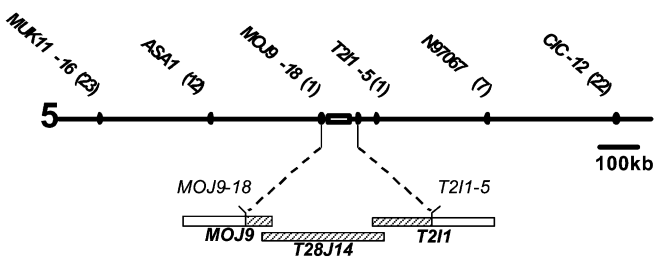


B

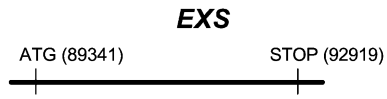


```
1     MAFLTALFLFLFFSFSSSAIVDLSSETTSLISFKRSLENPSLLSSWNVSSSASHCDWVGVTCLLGRVNSLSLPSLSLRGQIP  82
                                N- exs-2
83    KEISSLKNLRELCLAGNQFSGKIPPEIWNLKHLQTLDLSGNSLTGLLPSRLSELPELLYLDLSDNHFSGSLPLSFFISLPALS  165
166   SLDVSNNSLSGEIPPEIGKLSNLSNLYMGLNSFSGQIPSEIGNTSLLKNFAAPSCFFNGPLPKEISKLKHLAKLDLSYNPLK  247
                          STOP- exs-3
248   CSIPKSFGELQNLSILNLVSAELIGSIPPELGNCKSLKSLMLSFNSLSGPLPLELSEIPLLTFSAERNQLSGSLPSWIGKWKV  330
331   LDSLLLANNRFSGEIPREIEDCPMLKHLSLASNLLSGSIPRELCGSGSLEAIDLSGNLLSGTIEEVFDGCSSLGELLLTNNQI  413
414   NGSIPEDLWKLPLMALDLDSNNFTGEIPKSLWKSTNLMEFTASYNRLEGYLPAEIGNAASLKRLVLSDNQLTGEIPREIGK  494
495   LTSLSVLNLNANMFQGKIPVELGDCTSLTTLDLGSNNLQGQIPDKITALAQLQCLVLSYNNLSGSIPSKPSAYFHQIDMPD  575
576   LSFLQHHGIFDLSYNRLSGPIPEELGECLVLVEISLSNNHLSGEIPASLSRLTNLTILDLSGNALTGSIPKEMGNSLKLQGLN  658
659   LANNQLNGHIPESFGLLGSLVKLNLTKNKLDGPVPASLGNLKELTHMDLSFNNLSGELSSELSTMEKLVGLYIEQNKFTG  738
739   EIPSELGNLTQLEYLDVSENLLSGEIPTKICGLPNLEFLNLAKNNLRGEVPSDGVCQDPSKALLSGNKELCGRVVGSDCKI  819
820   EGTKLRSAWGIAGLMLGFTIIVFVFVFSLRRWVMTKRVKQRDDPERIEESRLKGFVDQNLYFLSGSRSREPLSINIAMFE  899
900   QPLLKVRLGDIVEATDHFSKKNIIGDGGFGTVYKACLPGEKTVAVKKLSEAKTQGNREFMAEMETLGKVKHPNLVSLLGY  979
980   CSFSEEKLLVYEYMVNGSLDHWLRNQTGMLEVLDWSKRLKIAVGAARGLAFLHHGFIPHIIHRDIKASNILLDGDFEPKVA  1060
1061  DFGLARLISACESHISTVIAGTFGYIPPEYGQSARATTKGDVYSFGVILLELVTGKEPTGPDFKESEGGNLVGWAIQKINQ  1141
                                                    E- exs-1
1142  GKAVDVIDPLLVSVALKNSQLRLLQIAMLCLAETPAKRPNMLDVLKALKEI                                  1192
```

C


Figure 5. Positional Cloning of the *EXS* Locus

(A) A summary of the fine mapping of the *EXS* locus. The black bar represents chromosome 5, and the short, vertical bars indicate the relative position of the markers used (the diagram is not drawn to scale). The number of recombination events identified in a total of 2234 chromosomes analyzed is indicated next to the name of the marker. The genetic interval containing the *EXS* locus is indicated by the dotted lines. The white and striped bars represent the P1 and BAC clones spanning the genetic interval: MOJ9 (Kazusa P1 clone, 86 kb), T28J14, and T2I1 (ESSA BAC clones, 104 kb and 117 kb, respectively). The short vertical bars indicate the position of the markers delimiting the genetic interval: *Moj9-8* is on the telomeric side, and *T2I1-5* is on the centromeric side. The *EXS* ORF has a single exon that spans positions 89341–92919 of *T24J18*.
(B) The predicted EXS protein sequence. The putative LRR domain is underlined with a single line, and the catalytic domain is underlined with a double line. The positions of the mutations in the three *exs* alleles are marked.
(C) A schematic representation of the EXS protein showing the approximate position of the mutations in the three *exs* alleles.

## Discussion

*EXS* encodes a putative serine/threonine LRR receptor kinase with highly specific, and apparently contrasting, roles in two structures — the anthers and the embryo of developing seeds. LRR receptor kinases have been implicated in various aspects of plant development, ranging from regulating meristem size (reviewed in [16]) to hormone perception [17–19] and general plant morphology [20, 21]. Although significant progress has been made in gathering molecular evidence for the role coreceptors play for some LRR receptors [18, 22–26], the mechanisms by which these signaling complexes operate in development are unknown. The observation that

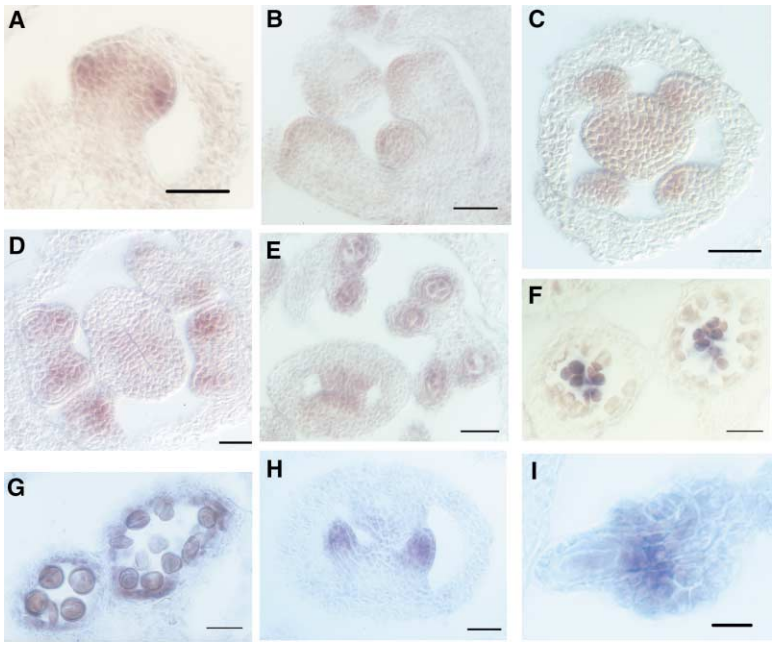


Figure 6. Expression of EXS in Wild-Type Inflorescences, Anthers, and Ovules as Shown by In Situ Hybridization

(A and B) A longitudinal section of inflorescence and floral meristems. *EXS* expression is detected at the flanks of the inflorescence meristem, in the positions of flower primordial initiation, and throughout the floral primordia.

(C–G) *EXS* expression in developing anthers. *EXS* transcripts are detected throughout anther primordia (C), although expression becomes restricted to the sporogenous cells and the anther wall layers as the anther develops (stage-8 and -9 buds [12]). (F and G) At the completion of meiosis and at the microspore stage, *EXS* transcripts are detected only in tapetal cells and in developing microspores.

(H) *EXS* is strongly expressed in developing ovule primordia.

(I) As development proceeds, high levels of *EXS* transcripts are detected in the chalazal region of ovules. No signal was observed when the sense *EXS* probe was used for in situ hybridization (results not shown).

The scale bar represents 50 μm in (A)–(H) and 20 μm in (I).

*EXS* acts to restrict development in the L2 of the anther and to enhance growth in the embryo suggests that *EXS* is capable of complexing with different partner molecules to regulate several developmental pathways. Such an interpretation is supported by the observation that a mutation of the EXS protein in a domain predicted to interact with other proteins (the LRR repeat region) exerts an extreme phenotype that is comparable to that of the predicted null mutant.

The young anther mutant phenotype points to *EXS* regulating cell division in the anther L2 layer through suppression of archesporial cell fate in all but four cells. How this is achieved is unclear, but were these cells to be specified first, perhaps as a result of their position, they might laterally inhibit the development of their neighbors in the L2. The part played by *EXS* in suppressing development of neighboring cells appears to be analagous to the role played by *CLAVATA* (*CLV1*) and its ligand *CLAVATA3* (*CLV3*) in controlling stem cell homeostasis at the shoot apical meristem. *CLV1* and *CLV3* operate in concert with a range of other genes, notably *WUSCHEL* (*WUS*), to establish a functional meristem (reviewed in [16]). *EXS* has no apparent role in meiosis, and the abortion of meiocytes in *exs* mutants most likely results from the absence of the tapetal and middle layers of the microsporangium. *EXS* transcripts are abundant in these layers, but it has yet to be proven that the gene plays a direct role in the specification of these cells types. Since the primary sporogenous cells must also participate in determining the cell fates in the radial microsporangium, particularly in the region adjacent to the connective, it remains plausible that the presence of extra sporogenous cells disrupts the signaling pathway regulating development in these cell layers. The fact that the *EXS* mutant phenotype involves an increase in numbers of one cell type at the apparent

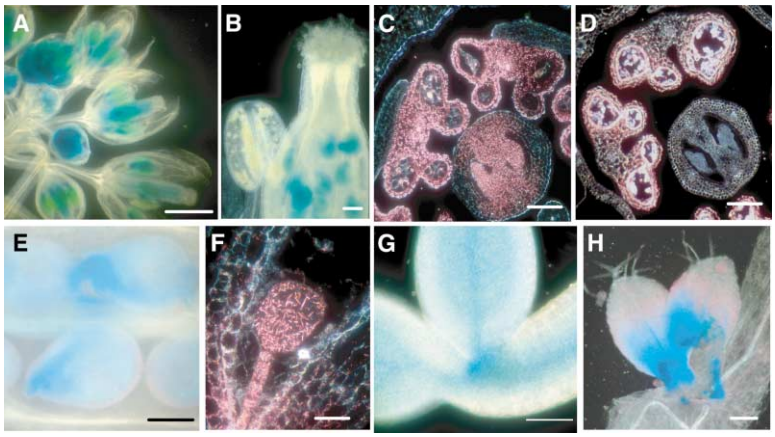


Figure 7. *EXS* Expression and EXS Localization as Detected by Transcriptional and Translational GUS Fusions

(A and B) Staining for *pEXS:GUS* expression in wild-type inflorescences. GUS activity is detected in developing anthers and ovules.

(C) A micrograph of a transverse section through a wild-type bud showing expression of the *pEXS:GUS* reporter gene in anthers and ovules.

(D) EXS protein localization in stage-10 wild-type buds. Expression of a *pEXS-EXS-GUS* translational fusion in an *exs-2* mutant plant. Anthers develop as in wild-type, indicating that the translational fusion is functional. Note the absence of the EXS protein in ovules.

(E–G) Expression of the *pEXS:GUS* reporter gene in (E and F) whole developing seeds and in (G) developing embryos.

(H) *pEXS:GUS* expression in the base of developing leaf primordia in a wild-type 7-day-old seedling.

The scale bar represents 400 μm in (A), 100 μm in (B), (E), and (H), and 50 μm in (C), (D), (G), and (H).

expense of another is intriguing and may point to the existence of factors that limit either cell numbers, or resources, within the anther.

The presence of *EXS* transcripts, but not EXS protein (as judged by translational fusions), in the developing ovule is interesting. Certainly, this protein may be rapidly turned over, but the fact that no female phenotype has been detected in *exs* mutants suggests that *EXS* is not required for ovular development. While the specification of a single archeosporial cell in ovule development must obviously require a different level of molecular control from events on the L2 of the anther, the observation that the *mac1* mutant in maize can form multiple megaspore mother cells [27] indicates that the opportunity for specification of extra archesporial cells also exists in ovules.

The anther and seed phenotypes are not easily aligned, for, in the seed, *EXS* is required not for suppressing development, but for enhancing cell size and the rate of embryonic development. Embryos homozygous for *exs* are strikingly reduced in size. In plants, organ size is controlled through an interplay between cell division and expansion (reviewed in [28]), and larger organs usually have more cells than smaller organs [29]. Hormones also play a key role in determining organ size, as evidenced by mutants overproducing ethylene that form smaller organs with fewer cells [30]. Conversely, disruption of the ethylene signaling pathway results in larger organs containing more larger cells [30]. Cell size alone can also be under hormonal control for gibberellic acid (GA), and brassinolides have been shown to regulate longitudinal cell expansion throughout the plant [31].

Control of organ and cell size is not solely under hormonal control, for transcription factors can affect these parameters. Mutations in *ANTEGUMENTA* (*ANT*), a member of the *AP2* transcription factor family, result in smaller organs containing fewer cells [32]. However, *EXS* specifically affects the size of the embryo by reducing cell size, without any accompanying affect on cell number. Also, unlike *ant* mutants, *exs* mutants show no aberrations in shoot growth, and overexpression of *EXS* results in no visible phenotype (data not shown), while *35S:ANT* plants possess enlarged organs containing more cells [33]. *exs* mutant plants are thus unusual in that, in the embryo only, smaller organs containing small cells are produced. The relationship between cell and organ size may be significant, but the fact that these embryos also develop slowly suggests that other factors may also contribute to the smaller final size of the embryo. This slow but normal development, and smaller cells of the *exs* embryos, point not to misregulation of stem cell number or fate, but rather to restricted growth of the cells themselves. The fact that *EXS* is expressed at all stages of embryogenesis but plays no apparent role in somatic postgermination development remains striking.

While this manuscript was under review, Zhao and coworkers [34] reported the isolation and characterization of *EXCESS MICROSPOROCYTES1* (*EMS1*). Although *EMS1* and *EXS* are clearly allelic, our interpretation of the mutant phenotype, and therefore of the role of the *EXS*/*EMS1* gene, differs in a number of important respects. *ems1* mutants are reported to differ from wild-type only once anther wall layer development is complete, and the authors attribute the increased number of sporogenous cells in mutant anthers to ISP cells adopting a sporogenous, rather than a tapetal, fate. We show here that, in the three available *exs* alleles, mutant anthers differ from wild-type anthers from the stage of archesporial division, and that a larger number of primary sporogenous cells are specified in mutant anthers. We also show that, in *exs* anthers, the final number of sporogenous cells is attained through a further division of these primary sporogenous cells prior to meiosis, an event that also occurs in wild-type anthers. Interestingly, Zhao et al. [34] report a persistence of the middle cell layer in *ems1* anthers; we found no evidence for the presence of a continuous middle cell layer in *exs* mutant plants, but rather rarely occurring, flattened cells with no defining morphology. These authors also report a failure of *ems1* mutant meiocytes to undergo cytokinesis, but, in *exs* anthers, cytokinesis clearly takes place, with mutant meiocytes degenerating shortly after the tetrad stage [4].

Importantly, while *EMS1* is reported to be anther specific, we found that *EXS* was expressed in a wide range of tissues, including inflorescence and floral meristems, developing anthers and ovules, and seeds. This expression of *EXS* in seeds is reflected by the clear embryo/seed phenotype of *exs* mutant lines; *ems1* mutants apparently have no such vegetative phenotype.

It is perhaps significant that *ems1* was isolated in a L*er* background, while the three *exs* alleles are in C24 lines. Some of the differences observed could certainly result from ecotypic variation.

## Experimental Procedures

### Plant Growth

*Arabidopsis* plants were grown on a mixture of Levingtons Compost and Vermiculite (3:1) in a Sanyo-Gallenkamp growth room at 20°C on an 18 hr light/6 hr dark cycle. All *exs* alleles are in the C24 background, and their origin is described in [4].

### Microscopy and Histological Staining

Specimens for light microscopy analysis were fixed, embedded in JB-4 glycol methacrylate resin, cut in 5 μm sections, and stained as described in Ruzin [35].

Feulgen-stained seeds for confocal laser microscopy were prepared according to a modified version of the protocol by Braselton et al. [36]. Whole siliques were cut at the ends and fixed in ethanol:acetic acid (3:1) for 3 hr, dehydrated through an ethanol series, and placed overnight in 100% ethanol. The samples were subsequently rehydrated, treated with 5 N HCl for 50 min, and stained with Schiff's reagent (Sigma S5133) for 2 hr. Before dehydration and embedding in Soft LR White Resin, the specimens were cleared for 1–2 days in a saturated chloral hydrate solution at room temperature. Samples were imaged with a Zeiss LSM 510 scanning microscope. Feulgen-stained specimens were excited with an argon ion laser at 488 nm, and emissions were detected at $<$515 nm.

Mature embryos stained with aniline blue for confocal microscopy were prepared as described in Bougourd et al. [37]. Samples were viewed with an argon ion laser at 514 nm excitation, 530 nm long pass filter. Embryo and cell size measurements were performed on collected images with the Carl Zeiss AIM LSM 5 Image Browser.

Samples for β-glucuronidase (GUS) staining were placed in 90% ice-cold acetone for 30 min, washed in staining buffer (100 mM Tris-HCl [pH 7.2], 50 mM NaCl, 0.1% Triton X-100), and incubated overnight at 37°C in buffer with 2 mM X-Gluc substrate, 1 mM potassium ferricyanide, and 1 mM potassium ferrocyanide. For whole-mount photography, stained samples were fixed in 4% paraformaldehyde and were cleared in saturated chloral hydrate solution for

a few hours. For light microscopy, specimens were fixed and embedded in JB-4 glycol methacrylate and were sectioned as described above.

### Mapping

Homozygous *exs* mutants in the C24 ecotype were crossed to Landsberg *erecta*, and the male sterile *exs* plants identified in the F2 population were used for mapping. Linkage analysis between the *exs* locus and genetic markers was detected with published SSLP and CAPS markers on a sample of 2234 recombinant chromosomes. *EXS* was placed on the top arm of chromosome 5, between the markers *CIC-12* (kindly provided by Scott Michaels) and *ASA1*. To further delineate the position of *EXS* within the *CIC-12-ASA1* interval, new CAPS markers were generated by using the published nucleotide sequence information (markers information available on request). These additional markers were used to identify proximal and distal recombination breakpoints in the mapping population and were used to place *EXS* in a genetic interval of 160 kb flanked by the CAPS markers *Moj9-16* and *T2I1-5*. The region was fully sequenced as part of the *Arabidopsis* Genome Initiative and was covered by a contig of three clones: the P1 clone *MOJ9*, and the BAC clones *T28J14* and *T2I1*. Genomic DNA representing all of the ORFs in this interval was amplified by PCR from wild-type C24 and from each of the three *exs* mutant alleles to identify mutant allele-specific restriction polymorphisms. Using this strategy, a *Hin*F1 polymorphism was detected between C24 and *exs-3* for an ORF representing a putative LRR Receptor Kinase. Sequence analysis of the LRR Receptor Kinase ORF from the mutant alleles *exs-1* and *exs-2* identified point mutations in the kinase and LRR domains, respectively. *EXS* cDNA was synthesized and amplified from C24 inflorescence RNA and was sequenced, and this confirmed that, as predicted by the annotation for this ORF, *EXS* contains a single exon coding for a protein of 1192 amino acids.

For the identification of the 3′ and 5′ UTR of EXS, total RNA was prepared from flower buds with a RNeasy Plant Mini Kit (Qiagen) according to the manufacturer's protocol.

3′ RACE cDNA was synthesized from inflorescence RNA by using the oligo d(T) anchor primer (5′-GACCACGCGTATCGATGTCGACTT TTTTTTTTTTTTTV-3′) according to the manufacturer's instructions (Roche). 3′ RACE products were amplified with the gene-specific primer EXS-31 (5′- ACCGGAGTATGGTCAGAGTGCC-3′) and the PCR anchor primer (5′-GACCACGCGTATCGATGTCGAC-3′); 1 ml of this PCR reaction was used in a second round of PCR with gene-specific primer EXS 32 (5′-CTGTGGATGTTATTGATCCACTG-3′) and the PCR anchor primer. The PCR products were cloned into *pGEM-T Easy* (Promega) and were sequenced. The 5′ UTR of *EXS* was amplified by direct PCR on cDNA synthesized from DNA-free total RNA. The primer used for direct amplification of the 5′ UTR was 5′-CTC TGCTCTTGTAAAAATTG-3′.

### Genetic Complementation and Plasmid Generation

A 9.2-kb SpeI genomic DNA fragment of Col-0 DNA, which included the *EXS* coding region, and 3.5 kb and 2.2 kb of the upstream and downstream sequences, respectively, was excised from the BAC *T28J14* (obtained from the *Arabidopsis* Biological Resource Center). The fragment was cloned into the unique XbaI site of the binary vector *pMLBART* [38]. The resulting plasmid was introduced into *Agrobacterium tumefaciens* GV3101 by electroporation, and, subsequently, the *Agrobacterium* culture was used to transform *exs-2/+* plants by the dipping inflorescences [39]. Male fertile plants were genotyped in the progeny of transformed plants by amplifying a *Tsp*509I polymorphism between Col-0 (of *T28J14*), wild-type C24, and the *exs-2* mutant allele. Those fertile plants that showed the codominant Col-0-specific 235-bp and the *exs-2*-specific 250-bp fragments, but lacked the 180-bp C24 wild-type band, confirmed complementation of *exs-2*.

To generate *35S:EXS* plants, the *EXS* ORF (including the stop codon) was amplified from *T28J14* with Pyrobest DNA Polymerase (TaKaRa) and gene-specific primers that introduced an XhoI site and a ClaI site at the 5′ and 3′ ends of the *EXS* ORF, respectively. PCR products were A-tailed, were cloned into *pGEM-T Easy* (Promega), and were sequenced to confirm that no errors were introduced in the *EXS* ORF. EXS cDNA was excised with ClaI and XhoI and were cloned into ClaI and XhoI sites of *pART7* [40], and the resulting *35S:EXS* fragment was excised from *pART7* with NotI and was cloned into a unique NotI site in *pMLBART*.

*pEXS-GUS* fusions were made by amplifying 1.9 kb of the 5′ upstream sequence of *EXS* (*pEXS*) and inserting it in pBlueScript II KS+ vector (Stratagene). The *uidA* cassette of pSLJ4K1 [41] was excised with ClaI and PstI and was cloned downstream of the *EXS* promoter. For the EXS-GUS translational fusion lines, the *EXS* promoter and ORF (lacking the stop codon) were cloned in frame upstream of the *GUS* cassette. The resulting fragments were excised with KpnI and SpeI and were cloned into the KpnI and XbaI sites of *pBJ36* [38], before transfer to *pMLBART*. All of the constructs were introduced into *Agrobacterium tumefaciens* GV3101 by electroporation and were transformed into *exs-2/+* plants by dipping inflorescences [39]. Transformants were genotyped by using the *Tsp*509I CAPS as described above.

### RT-PCR Analysis and In Situ Hybridization

Total RNA was isolated in different tissues by using the RNeasy Plant Mini Kit (Qiagen) according to the manufacturer's instructions; all RNA samples were treated with RNase-free DNase (Promega) prior to cDNA synthesis. RT-PCR analysis was performed on cDNA synthesized from total RNA isolated from different tissues, and *EXS* cDNA was amplified with specific primers (forward primer: 5′-CCTT CTCTAAAAGAACATGGCG-3′; reverse primer: 5′-CTCCTTAAGAGC CTTCAACAC-3′). *EXS* cDNA was sequenced and identified a single exon that encodes a predicted protein of 1192 amino acids. For RT-PCR analysis, and to generate *EXS* probes for in situ hybridization, the first 330 bp of the *EXS* ORF were amplified with specific primers (forward primer: 5′-AAAACCCATCTCTCCTTTCTTC-3′; reverse primer: 5′-ACGATAGAGGAAGTGAACCG-3′). Sequence analysis of the *EXS* in situ probe confirmed that it does not show homology to other sequences in the *Arabidopsis* genome and hence is likely to be specific for *EXS*. In situ hybridization was carried out according to Jackson et al. [42]. The same primers used for the RT-PCR analysis were used for probe generation.

### Acknowledgments

We thank all members of the Dickinson group, in particular Shilpa Ghelani for invaluable technical support, Melissa Spielman for her advice on microscopy and for thoughtful comments to the manuscript, and Jose Gutierrez-Marcos for helpful discussions. We thank Andrey Lagodienko for help with plants, Qing Zhang for sequencing, and John Baker for his assistance with photography. We thank Miltos Tsiantis for valuable discussions and constructive advice. We are very grateful to Ned Friedman for discussions and advice on light microscopy. We thank John Bowman for the gift of plasmids and Scott Michaels for sharing unpublished marker information. We thank Yaron Levy, Thierry Desnos, and Antony Gendall for their advice with mapping. This work was made possible by funding from the Biotechnology and Biological Sciences Research Council.

Received: July 30, 2002
Revised: August 15, 2002
Accepted: August 15, 2002
Published: October 15, 2002

### References

1. Schiefthaler, U., Balasubramanian, S., Sieber, P., Chevalier, D., Wisman, E., and Schneitz, K. (1999). Molecular analysis of NOZZLE, a gene involved in pattern formation and early sporogenesis during sex organ development in *Arabidopsis thaliana*. Proc. Natl. Acad. Sci. USA *96*, 11664–11669.
2. Yang, W.C., Ye, D., Xu, J., and Sundaresan, V. (1999). The SPOROCYTELESS gene of *Arabidopsis* is required for initiation of sporogenesis and encodes a novel nuclear protein. Genes Dev. *13*, 2108–2117.
3. Bhatt, A.M., Canales, C., and Dickinson, H.G. (2001). Plant meiosis: the means to 1N. Trends Plant Sci. *6*, 114–121.
4. Sorensen, A., Guerineau, F., Canales-Holzeis, C., Dickinson, H.G., and Scott, R.J. (2002). A novel extinction screen in *Arabi-*

*dopsis thaliana* identifies mutant plants defective in early microsporangial development. Plant J. *29*, 581–594.

5. Balasubramanian, S., and Schneitz, K. (2000). NOZZLE regulates proximal-distal pattern formation, cell proliferation and early sporogenesis during ovule development in *Arabidopsis thaliana*. Development *127*, 4227–4238.
6. Skinner, D.J., Baker, S.C., Meister, R.J., Broadhvest, J., Schneitz, K., and Gasser, C.S. (2001). The *Arabidopsis* HUELLENLOS gene, which is essential for normal ovule development, encodes a mitochondrial ribosomal protein. Plant Cell *13*, 2719–2730.
7. Gross-Hardt, R., Lenhard, M., and Laux, T. (2002). WUSCHEL signaling functions in interregional communication during *Arabidopsis* ovule development. Genes Dev. *16*, 1129–1138.
8. Byzova, M.V., Franken, J., Aarts, M.G.M., de Almeida-Engler, J., Engler, G., Mariani, C., Campagne, M.M.V., and Angenent, G.C. (1999). *Arabidopsis* STERILE APETALA, a multifunctional gene regulating inflorescence, flower, and ovule development. Genes Dev. *13*, 1002–1014.
9. Hauser, B.A., He, J.Q., Park, S.O., and Gasser, C.S. (2000). TSO1 is a novel protein that modulates cytokinesis and cell expansion in *Arabidopsis*. Development *127*, 2219–2226.
10. Liu, Z.C., Running, M.P., and Meyerowitz, E.M. (1997). TSO1 functions in cell division during *Arabidopsis* flower development. Development *124*, 665–672.
11. Sanders, P.M., Bui, A.Q., Weterings, K., McIntire, K.N., Hsu, Y.C., Lee, P.Y., Truong, M.T., Beals, T.P., and Goldberg, R.B. (1999). Anther developmental defects in *Arabidopsis thaliana* male-sterile mutants. Sexual Plant Reproduction *11*, 297–322.
12. Bowman, J. (1994). *Arabidopsis*, An Atlas of Morphology and Development (New York: Springer-Verlag).
13. Davis, G.L. (1966). Systematic Embryology of the Angiosperms (New York: John Wiley and Sons).
14. Klimyuk, V.I., and Jones, J.D.G. (1997). AtDMC1, the *Arabidopsis* homologue of the yeast DMC1 gene: characterization, transposon-induced allelic variation and meiosis-associated expression. Plant J. *11*, 1–14.
15. Paul, W., Hodge, R., Smartt, S., Draper, J., and Scott, R. (1992). The isolation and characterization of the tapetum-specific *Arabidopsis thaliana* A9 gene. Plant Mol. Biol. *19*, 611–622.
16. Clark, S.E. (2001). Cell signalling at the shoot meristem. Nat. Rev. Mol. Cell Biol. *2*, 276–284.
17. Li, J.M., and Chory, J. (1997). A putative leucine-rich repeat receptor kinase involved in brassinosteroid signal transduction. Cell *90*, 929–938.
18. He, Z.H., Wang, Z.Y., Li, J.M., Zhu, Q., Lamb, C., Ronald, P., and Chory, J. (2000). Perception of brassinosteroids by the extracellular domain of the receptor kinase BRI1. Science *288*, 2360–2363.
19. Wang, Z.Y., Seto, H., Fujioka, S., Yoshida, S., and Chory, J. (2001). BRI1 is a critical component of a plasma-membrane receptor for plant steroids. Nature *410*, 380–383.
20. Torii, K.U., Mitsukawa, N., Oosumi, T., Matsuura, Y., Yokoyama, R., Whittier, R.F., and Komeda, Y. (1996). The *Arabidopsis* ERECTA gene encodes a putative receptor protein kinase with extracellular leucine-rich repeats. Plant Cell *8*, 735–746.
21. Lease, K.A., Lau, N.Y., Schuster, R.A., Torii, K.U., and Walker, J.C. (2001). Receptor serine/threonine protein kinases in signalling: analysis of the erecta receptor-like kinase of *Arabidopsis thaliana*. New Phytologist *151*, 133–143.
22. Fletcher, L.C., Brand, U., Running, M.P., Simon, R., and Meyerowitz, E.M. (1999). Signaling of cell fate decisions by CLAVATA3 in *Arabidopsis* shoot meristems. Science *283*, 1911–1914.
23. Brand, U., Fletcher, J.C., Hobe, M., Meyerowitz, E.M., and Simon, R. (2000). Dependence of stem cell fate in *Arabidopsis* on a feedback loop regulated by CLV3 activity. Science *289*, 617–619.
24. Yu, L.P., Simon, E.J., Trotochaud, A.E., and Clark, S.E. (2000). POLTERGEIST functions to regulate meristem development downstream of the CLAVATA loci. Development *127*, 1661–1670.
25. Schoof, H., Lenhard, M., Haecker, A., Mayer, K.F.X., Jurgens, G., and Laux, T. (2000). The stem cell population of *Arabidopsis* shoot meristems is maintained by a regulatory loop between the CLAVATA and WUSCHEL genes. Cell *100*, 635–644.
26. Wang, Z.Y., Nakano, T., Gendron, J., He, J.X., Chen, M., Vafeados, D., Yang, Y.L., Fujioka, S., Yoshida, S., Asami, T., et al. (2002). Nuclear-localized BZR1 mediates brassinosteroid-induced growth and feedback suppression of brassinosteroid biosynthesis. Dev. Cell *2*, 505–513.
27. Sheridan, W.F., Golubeva, E.A., Abrhamova, L.I., and Golubovskaya, I.N. (1999). The mac1 mutation alters the developmental fate of the hypodermal cells and their cellular progeny in the maize anther. Genetics *153*, 933–941.
28. Mizukami, Y. (2001). A matter of size: developmental control of organ size in plants. Curr. Opin. Plant Biol. *4*, 533–539.
29. Niklas, K.J. (1994). Plant Allometry: The Scaling of Form and Process (Chicago: The University of Chicago Press).
30. Ecker, J.R. (1995). The ethylene signal-transduction pathway in plants. Science *268*, 667–675.
31. Shibaoka, H., and Nagai, R. (1994). The plant cytoskeleton. Curr. Opin. Plant Biol. *6*, 10–15.
32. Mizukami, Y., and Fischer, R.L. (2000). Plant organ size control: AINTEGUMENTA regulates growth and cell numbers during organogenesis. Proc. Natl. Acad. Sci. USA *97*, 942–947.
33. Krizek, B.A. (1999). Ectopic expression AINTEGUMENTA in *Arabidopsis* plants results in increased growth of floral organs. Dev. Genet. *25*, 224–236.
34. Zhao, D.-Z., Wang, G.-F., Speal, B., and Ma, H. (2002). The *EXCESS MICROSPOROCYTES1* gene encodes a putative leucine-rich repeat receptor protein kinase that controls somatic and reproductive cell fates in the *Arabidopsis* anther. Genes Dev. *16*, 2021–2031.
35. Ruzin, S.E. (1999). Plant Microtechnique and Microscopy (Oxford: Oxford University Press).
36. Braselton, J.P., Wilkinson, M.J., and Clulow, S.A. (1996). Feulgen staining of intact plant tissues for confocal microscopy. Biotech. Histochem. *71*, 84–87.
37. Bougourd, S., Marrison, J., and Haseloff, J. (2000). An aniline blue staining procedure for confocal microscopy and 3D imaging of normal and perturbed cellular phenotypes in mature *Arabidopsis* embryos. Plant J. *24*, 543–550.
38. Eshed, Y., Baum, S.F., Perea, J.V., and Bowman, J.L. (2001). Establishment of polarity in lateral organs of plants. Curr. Biol. *11*, 1251–1260.
39. Clough, S.J., and Bent, A.F. (1998). Floral dip: a simplified method for Agrobacterium-mediated transformation of *Arabidopsis thaliana*. Plant J. *16*, 735–743.
40. Gleave, A.P. (1992). A versatile binary vector system with a T-DNA organizational structure conducive to efficient integration of cloned DNA into the plant genome. Plant Mol. Biol. *20*, 1203–1207.
41. Jones, J.D., Shlumukov, L., Carland F., English, J., Scofield, S.R., Bishop, G.J., and Harrison, K. (1992). Effective vectors for transformation, expression of heterologous genes, and assaying transposon excision in transgenic plants. Transgenic Res. *1*, 285–297.
42. Jackson, D.P. (1992). In Situ Hybridisation in Plants (Oxford: IRL Press/Oxford University Press).